NANO LETTERS

2006
Vol. 6, No. 11
2626−2629

Sub-20-nm Alignment in Nanoimprint Lithography Using Moiré Fringe

Nianhua Li,* Wei Wu, and Stephen Y. Chou*

NanoStructure Laboratory, Department of Electrical Engineering, Princeton University, Princeton, New Jersey 08544

Received February 14, 2006; Revised Manuscript Received August 2, 2006

ABSTRACT

Accurate multi-level overlay capability for nanoimprint lithography (NIL) is essential to integrated circuit manufacturing and other multilayer imprint applications. Using the "beat" grating image (Moiré fringe) generated by overlaying two sets of gratings that have slightly different periods, we obtained an alignment signal with a sensitivity better than 10 nm in nanoimprint lithography. The alignment signal is, as expected, independent of the size of the gap between the wafer and the imprint mold. We achieved a single-point overlay accuracy (error distribution) of sub-20 nm between the first and second imprinted layers by using two sets of Moiré fringes. With higher precision nanopositioning stages, better single-point alignment accuracy is expected. Furthermore, we achieved sub-150 nm alignment over an area of 1 sq in and sub-250 nm over the entire area of a 4 in wafer using simple low-resolution stages without temperature control or wafer–mold mismatch compensation. With better stages, precision temperature control, and wafer–mold mismatch compensation, we believe that much higher overlay alignment accuracy over large areas (either in a 1 sq in die or a full wafer) is feasible.

Since its origination in 1995,[1] nanoimprint lithography (NIL) has found its way to applications in many disciplines where patterning of nanostructures is needed, such as subwavelength optics, single electron and quantum devices, molecular and bioelectronics, nanomagnetic devices, and nanobio sensors. One of the most important potential applications of NIL is the manufacturing of integrated circuits (ICs). The superb resolution (6 nm has been demonstrated[2]) and potential low cost make NIL an attractive candidate for the next generation of lithography tools for IC manufacturing nodes of 32 nm and beyond. In fact, nanoscale transistors in Si[3−5] and in organic/polymeric materials[6,7] have been fabricated using NIL technology. But for IC manufacturing, high resolution alone is insufficient; one must achieve sub-30 nm overlay alignment accuracy in addition to low defect density and high throughput.[8]

Several works in NIL alignments have been reported.[3,9,10] Fabrication of nanoMOSFETs over 4 in using NIL at all lithography levels (four layers: active, gate, contact holes, and metal) with sub-500 nm overlay alignments has been demonstrated.[3] However, for state-of-the art IC manufacturing, sub-30 nm alignment accuracy is required. In projection steppers, this precision is achieved by dynamically detecting the intensity of the alignment signal from alignment marks on the substrate and reticle.[11] But it is difficult to implement this method in a proximity/contact lithography system like NIL, where the mask and substrate are not only close to each other but also being moved toward each other and being in contact, as opposed to a projection stepper where the mask and substrate are separated by lenses. For achieving high overlay accuracy in proximity lithography, several novel techniques have been used. Flanders and Smith[12] and Uchida et al.[13] used the Moiré technique by overlapping gratings with equal periods on mask and substrate and detecting the alignment signal by comparing the intensities of different diffraction beams. Murnane superimposed two sets of gratings with different periods on the mask and substrate, resulting in a Moiré pattern whose period scales inversely with the difference between the periods of the original patterns.[14] Alignment information was derived from the Moiré pattern. Moel et al. and Moon et al. used similar alignment mark patterns with broadband light illumination.[15,16] A computer-based digital-image-processing technique was used to obtain alignment information and determine alignment. Zhou et al.[17] and Chen et al.[18] used a Fresnel zone plate on the mask to focus a light beam on a diffracting pattern on the substrate and obtain the alignment signal from the diffracted light beam. When NIL originated in 1995, using a Moiré pattern for NIL overlay alignment was also conceived.[19]

Overlay in NIL is different from that in proximity lithography. In proximity lithography, one can fix the gap between the wafer and the mask and then perform the alignment. In NIL, one needs to do alignment while bringing the mold in contact with the resist on the wafer and imprint into it. Hence, for NIL alignment, we need an accurate method that does not depend on the gap between the mold and substrate because this gap is changing from tens of

* Corresponding authors. E-mail: chou@princeton.edu; nli@princeton.edu.

10.1021/nl0603395 CCC: $33.50
Published on Web 09/30/2006

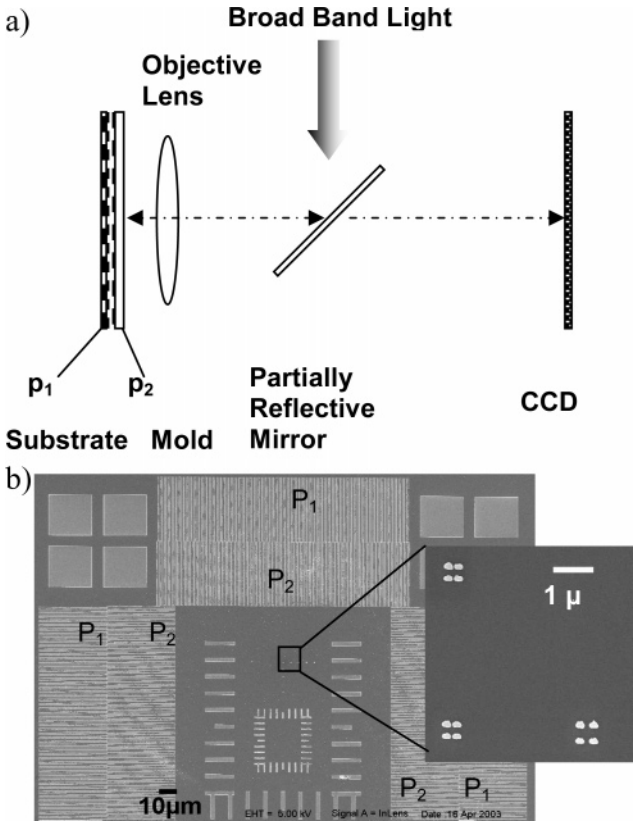

Figure 1. (a) Schematic of alignment system setup. Broadband illumination is projected onto the mold/substrate, and the diffraction from the gratings on the mold/substrate is collected by objective lens and imaged onto CCD through optics (not shown). (b) SEM image of alignment marks on the substrate. Two sets of boxes are at the upper corners. Three pairs of gratings with periods p_1 and p_2 are at the two sides and the top. The center of the image contains tiny boxes (inset: zoom in) that are used to check the result of alignment.

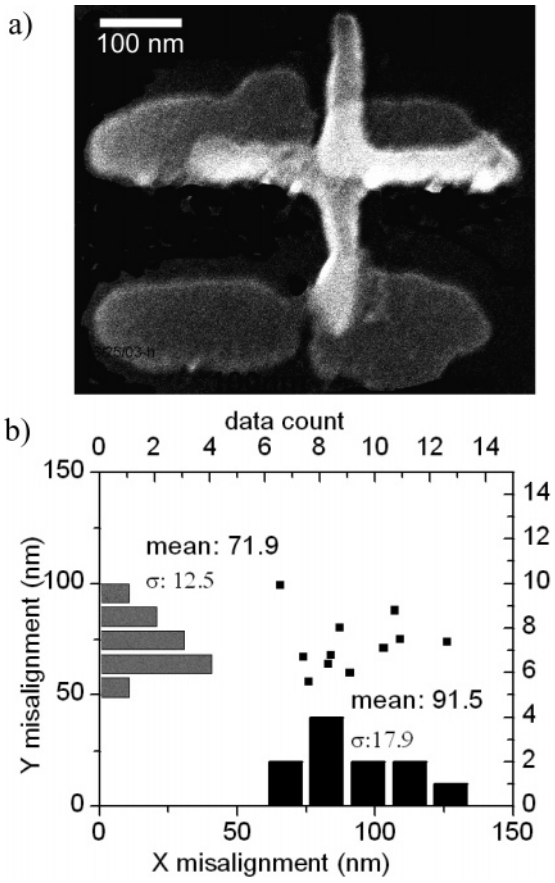

Figure 2. (a) SEM image of two sets of alignment marks (four boxes for the first layer and a cross for the second layer). When aligned perfectly, the cross should be at the center of the four boxes (distorted due to EBL proximity effect). (b) Statistics of misalignment. The average misalignment is 80 nm with standard deviation less than 20 nm in both the x and y directions.

micrometers to zero during the imprint process and may not be uniform over the whole substrate because of substrate non-flatness. In this paper, we describe our alignment method for NIL with a demonstrated sub-10-nm alignment sensitivity, sub-20-nm, sub-250-nm, and sub-500-nm alignment accuracy between two layers for a single point, 1 sq in area, and 4 in wafer area, respectively.

When two sets of gratings with slightly different periods, p_1 and p_2, are superimposed under illumination, a "beat" grating image (Moiré fringe) will form because of the obstruction of two geometric light beams. This Moiré fringe has a period of $P = p_1 \times p_2/(p_1 - p_2)$, which is much larger than both p_1 and p_2, hence magnifying of the original period by a factor of about $p_1/(p_1 - p_2)$. This amplification can be used to detect a minute relative shift between the two layers of gratings with accuracy in the nanometer range. When p_1 and p_2 have dimensions comparable to the light wavelength of interest, diffraction and interference have to be considered to derive the above relation. As depicted in Figure 1a, incident light is diffracted by gratings p_1 and p_2, and imaged by a lens, forming Moiré fringes on the CCD image plane.

The Moiré fringes are particularly well suited to NIL. A diffraction analysis shows that the periods and locations of the Moiré fringes do not depend on the gap between the two gratings, nor the wavelength of the illumination. This means that we can use the Moiré fringes for an accurate alignment during an imprint process without worrying about the changing gap between mold and substrate. It also means that we can use white-light illumination for accurate Moiré fringes.

In our experiments, the alignment marks are the grating periods $p_1 = 1\ \mu$m and $p_2 = 0.95\ \mu$m, forming a magnification factor of 20. To further improve Moiré fringe precision, we put both gratings p_1 and p_2 side by side on the substrate (shown in Figure 1b and the complementary mark of p_2 and p_1 on the NIL mask. When the substrate and the mask overlap, two sets of Moiré fringes are formed side by side (Figure 3a), which move in opposite directions during the movement of the substrate relative to the mold, therefore enhancing the magnification in overlay alignment accuracy by another factor of 2. The alignment marks are designed so that the mold and substrate are aligned only when the two sets of Moiré fringes are aligned with each other. However, the alignment of Moiré fringes does not guarantee the alignment of the mold and substrate because the Moiré fringe repeats itself when the mold and substrate are offset by a base period. To eliminate the ambiguity, traditional optical alignment marks of the crosses and boxes, as well

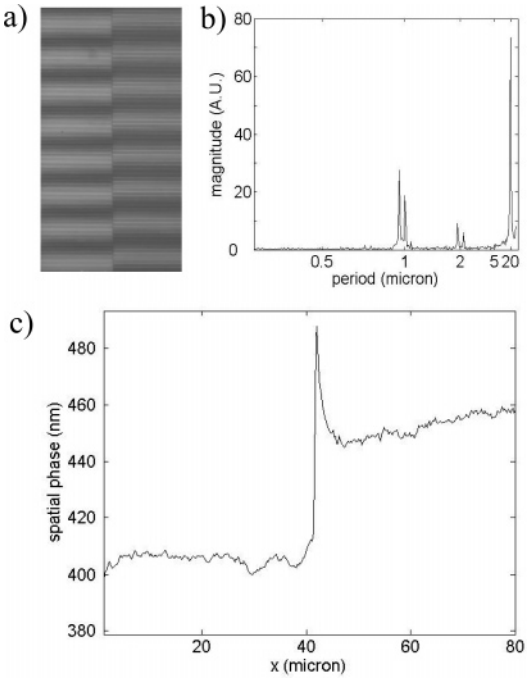

Figure 3. (a) Optical image of two sets of Moiré fringe side by side. (b) Spatial frequency spectrum of the Moiré fringe. The main peak around 20 μm is the peak for Moiré fringe. The double peaks around 1 μm are the two base gratings. (c) Spatial phase as a function of location. The standard deviation at each side is less than 7 nm.

as verniers, are put on the substrate and the mask beside the grating marks. The combination of these alignment marks ensures a unique position for alignment of the mask and the substrate. Furthermore, additional fine verniers and cross/box marks with dimensions of 50 nm are put alongside the alignment marks (Figure 1b inset), serving as the check marks for SEM evaluation of the precision of alignment accuracy after an imprint is done. These tiny patterns are barely visible with an optical microscope during alignment. The substrates used are silicon or fused silica with a 20 nm chrome pattern. The mask material is fused silica coated with 100-nm-thick silicon nitride (SiN_x). The topographical pattern is etched in the SiN_x layer. The top of the SiN_x pattern is coated with a 10-nm-thick layer of chrome. This chrome layer is used as a SiN_x etching mask and also helps to increase optical contract during alignment.

The experiment was carried out with a commercial mask aligner that has simple manual stages. An optical microscope with maximum magnification of 20× (NA = 0.40) and CCD cameras were used to capture the images of both coarse alignment marks and the Moiré pattern. Broadband illumination was brought to alignment marks through objective lenses by optical fiber from the lamp housing. Alignment was done by hand/eye coordination of the aligner operator. An imprint resist with a thickness of 80−120 nm was spin coated on the substrate. During alignment and imprint, the aligner first closed the gap between the mold and substrate to about 20 μm. A coarse alignment was performed using the cross/boxes and vernier pattern, to better than 1 μm accuracy. Then the gap between mold and substrate was further reduced below 10 μm, where Moiré fringes became clearly visible. Fine aligning was adjusted according to the Moiré fringes. When aligned, the substrate was brought closer to the mold, while monitoring the Moiré fringes carefully, adjusting the position of the substrate when necessary. Because the vertical motion of the substrate toward the mold often results in a lateral shift, fine alignment has to be adjusted carefully several times before the mold and substrate finally come into contact. Even when the patterns on the mold are fully immerged in imprint resist after contact, the Moiré fringes and other alignment marks are still clearly visible because the top of the alignment pattern on our mold is coated with opaque chromium and SiN_x, the material composing the mold pattern itself, has a reddish tint under optical microscope. After curing the resist, the mold and substrate were separated. The alignment result was checked by optical and scanning electron microscopy.

In testing the overlay accuracy, we tested alignment accuracy at a single point first and then between two points over a certain field size. The alignment accuracy at a single point is a direct measurement of the alignment method and the accuracy of the stages, whereas the alignment accuracy of two points includes the additional effects of temperature nonuniformity, thermal expansion difference between the substrate and the mold, and the mismatch of the mask and substrate patterns.

The overlay alignment accuracy was judged by SEM measurements of the alignment of the cross and the box marks (Figure 1b inset). For a perfect alignment, the cross should be located at the center of the four boxes. A misalignment was characterized by the distance from the center of the boxes to the center of the cross. Figure 2a shows a typical image of the cross mark and box mark (note the distortion of the four boxes due to the proximity effect of electron beam lithography (EBL) that created the marks). The average misalignment for a single point (Figure 2b) is 80 nm. The standard deviation (σ) of the misalignment is below 20 nm in both the x and y directions. The relatively large average misalignment (80 nm) was a systematic error due to the relative pattern placement error of the molds used for the two layers of lithography, which can be readily corrected by more precisely fabricated molds. Although reducing the pattern placement error in multilayer lithography masks is critical to reduce the alignment error and numerous works has addressed it, we focus on the study of issues in alignment for a given set of masks, rather than improvement of the mask accuracy itself. The 20 nm distribution is the real uncertainty in our alignment method.

The 20 nm alignment uncertainty comes mainly from our stage accuracy because our Moiré detection system allows us to see 7 nm misalignment, as discussed below. In our setup, although the human eye can detect, for example, 1/10 of the Moiré fringe period due to misalignment, which corresponds to 1/20 of base grating period, namely, about 50 nm, computer-aided image processing offers much better sensitivity on detecting misalignment. Figure 3a is the optical picture of an actual Moiré fringe formed after imprint. Figure 3b and c are its Fourier transforms. The difference in spatial phase of the two sides reflects the fact that the two sets of Moiré fringe are not aligned. As shown, the noise level

a)

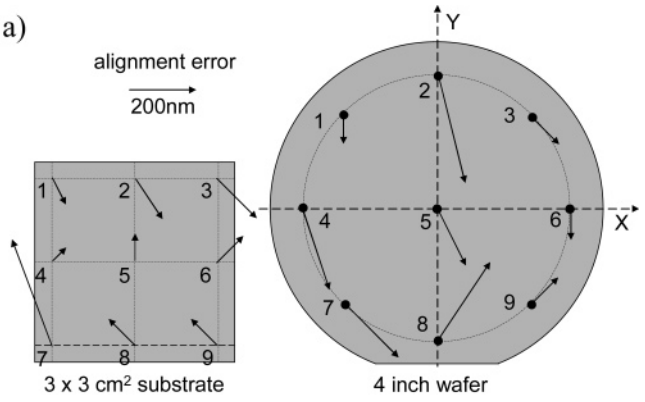

b)

sample #		site / align error (nm)	1	2	3	4	5	6	7	8	9	ave.
4 inch wafer	1	δx	0	80	80	80	80	0	160	160	80	80
		δy	-80	-320	-80	-240	-160	-80	-160	240	80	-88.9
		$(\delta x^2+\delta y^2)^{1/2}$	80	330	113	253	179	80	226	288	113	185
	2	δx	80	160	80	0	-120	120	-80	280	-560	-4.44
		δy	240	0	-240	120	160	80	0	-400	240	22.2
		$(\delta x^2+\delta y^2)^{1/2}$	253	160	253	120	200	144	80	488	609	256
	3	δx	160	80	160	-160	0	0	-240	-160	0	-17. 8
		δy	80	80	-160	-320	-160	-240	0	-80	-80	-97. 8
		$(\delta x^2+\delta y^2)^{1/2}$	179	113	226	358	160	240	240	179	80	197
3cm x 3cm substrate	1	δx	40	80	120	40	0	80	-120	-80	-80	8.89
		δy	-80	-120	-120	40	80	80	160	80	80	22.2
		$(\delta x^2+\delta y^2)^{1/2}$	89.4	144	170	56.6	80	113	200	113	113	120
	2	δx	0	-160	-160	-80	-80	-80	-120	-160	-80	-102
		δy	-40	-40	-80	-120	-40	-120	-120	-120	-40	-80
		$(\delta x^2+\delta y^2)^{1/2}$	40	165	179	144	89	144	170	200	89.4	136
	3	δx	-80	80	80	-120	-40	-80	-120	-160	-40	-53.3
		δy	80	-120	-160	0	-80	-160	-120	-80	80	-62.2
		$(\delta x^2+\delta y^2)^{1/2}$	113	144	179	120	89	179	170	179	89.4	140

Figure 4. (a) Typical alignment map for 1 in substrate and 4 in wafer. (b) Statistics of alignment on 1 in and 4 in substrate, with 9 measurement sites on each sample and 3 samples for each size of substrates.

(standard error) of the spatial phase is below 7 nm, which is the limit for detecting the misalignment in our current system. However, our aligner stage used in the experiment has an accuracy of 100 nm, which is the limiting factor of the current alignment experiment.

In our study of the alignments over different areas (1 sq in and a full 4 in wafer area), nine points in the imprinted area of a substrate were measured relative to underlying pattern to decide an overlay alignment of the substrate in the *x*, *y*, and rotation directions (Figure 4). The alignment error on a point $((\Delta x^2 + \Delta y^2)^{1/2})$ was averaged over the nine points to get misalignment measure for the sample. The average misalignment for three typical samples is about 130 nm for 1 in sq area die and 250 nm for a full 4 in wafer, respectively.

A close examination the alignment errors (Δx, Δy) at each point shows that they vary from point to point in a rather random fashion. Such alignment errors can come from several sources, including the errors in placing the patterns on the mask, the error in placing the first layer patterns on the substrate, local temperature variation, and local variation of stress (hence related distortions) on the mask or the substrate during imprinting. The factors must be dealt with care in the manufacturing with good alignment needs.

In conclusion, a broadband illumination Moiré-fringe-based mold−substrate aligning scheme demonstrated a sensitivity better than 7 nm. The alignment signal does not depend on the gap between mold and substrate and remains measurable throughout and after the whole imprint process. With this method, we achieved an accuracy of 20 nm for single point alignment, sub-150 nm alignment for a 1 in area die, and sub-250 nm for a full 4 in wafer. The high sensitivity in the Moiré fringe can also be used to help the identification and correction of the alignment errors caused by pattern misplacement, local temperature fluctuation, and local imprint stress variations (hence distortions).

Acknowledgment. We thank Dr. Haixiong Ge for the imprint resist. Photronics Inc. provided some of the photo and imprint masks. This work is supported in part by DARPA and ONR.

References

(1) Chou, S. Y.; Krauss, P. R.; Renstrom, P. J. *Appl. Phys. Lett.* **1995**, *67*, 3114−3116.
(2) Austin, M. D.; Zhang, W.; Ge, H. X.; Wasserman, D.; Lyon, S. A.; Chou, S. Y. *Nanotechnology* **2005**, *16*, 1058−1061.
(3) Zhang, W.; Chou, S. Y. *Appl. Phys. Lett.* **2003**, *83*, 1632−1634.
(4) Martini, I.; Dechow, J.; Kamp, M.; Forchel, A.; Koeth, J. *Microelectron. Eng.* **2002**, *60*, 451−455.
(5) Guo, L. J.; Krauss, P. R.; Chou, S. Y. *Appl. Phys. Lett.* **1997**, *71*, 1881−1883.
(6) Austin, M. D.; Chou, S. Y. *Appl. Phys. Lett.* **2002**, *81*, 4431−4433.
(7) McAlpine, M. C.; Friedman, R. S.; Lieber, D. M. *Nano Lett.* **2003**, *3*, 443−445 APR 2003.
(8) Austin, M. D.; Ge, H.; Wu, W.; Wasserman, D.; Lyon, S.; Chou, S. Y. Fabrication of 5 nm line width and 14 nm pitch features by nanoimprint lithography. In *Second International Conference on Nanoimprint and Nanoprint Technology*.
(9) Alkaisi, M. M.; Jayatissa, W.; Konijn, M. *Curr. Appl. Phys.* **2004**, *4*, 111−114.
(10) Fuchs, A.; Vratzov, B.; Wahlbrink, T.; Georgiev, Y.; Kurz, H. *J. Vac. Sci. Technol., B* **2004**, *22*, 3242−3245.
(11) Wittekoek, S.; van den Brink, M.; Linders, H.; Stoeldrayer, J.; Martens, J. W. D.; Ritchie, D. 534 *SPIE* Vol. 1264 Optical/Laser Microlithography III, 1990.
(12) Flanders, D. C.; Smith, H.; Austin, S. *Appl. Phys. Lett.* **1977**, *31*, 426−428.
(13) Uchida, Y.; Hattori, S.; Nomura, T. *J. Vac. Sci. Technol., B* **1987**, *5*, 244−247.
(14) Murnane, M. R.; Raymond, C. J.; Hatab, Z. R.; Naqvi, S. S. H.; McNeil, J. R. *Proc. SPIE* **1994**, *2196*, 47.
(15) Moel, A.; Moon, E. E.; Frankel, R. D.; Smith, H. I. *J. Vac. Sci. Techonol., B* **1993**, *11*, 2191−2194.
(16) Moon, E. E.; Everett, P. H.; Smith, H. I. *J. Vac. Sci. Technol., B* **1995**, *13*, 2648−2652.
(17) Zhou, H.; Feldman, M.; Bass, R. *J. Vac. Sci. Technol., B* **1994**, *12*, 3261−3264.
(18) Chen, G.; Wallace, J. P.; Cerrina, F. *Jpn. J. Appl. Phys., Part 1* **1993**, *32*, 5977−5981.
(19) Chou, S. Y. Nanoimprint lithography. U.S. Patent 5,772,905, 1998.

NL0603395